Acta Crystallographica Section D
Biological Crystallography
ISSN 0907-4449

Crystallization and preliminary X-ray crystallographic analysis of the Hsp100 chaperone ClpB from *Thermus thermophilus*

Sukyeong Lee,[a] Makyio Hisayoshi,[b] Masasuke Yoshida[b] and Francis T. F. Tsai[a]*

[a]Verna and Marrs McLean Department of Biochemistry and Molecular Biology, Baylor College of Medicine, Houston, TX, USA, and [b]Chemical Resources Laboratory, Tokyo Institute of Technology, Yokohama 226-8503, Japan

Correspondence e-mail: ftsai@bcm.tmc.edu

Received 7 October 2003
Accepted 15 October 2003

ClpB from *Thermus thermophilus* (*T*ClpB) has been crystallized by the vapour-diffusion method in the presence of adenosine 5′-(β,γ-imido)triphosphate (AMPPNP) and adenosine 5′-(γ-thio)triphosphate (ATPγS), respectively. Complete native data sets have been collected from frozen crystals, which belonged to the primitive orthorhombic space group $P2_12_12_1$ with unit-cell parameters a = 109.2, b = 139.6, c = 213.0 Å, $\alpha = \beta = \gamma = 90^\circ$.

1. Introduction

Bacterial ClpB and its yeast orthologue heat-shock protein 104 (Hsp104) are ATP-dependent molecular chaperones which form large ring structures and belong to the Clp/Hsp100 family of ATPases associated with diverse cellular activities (AAA^+; Schirmer *et al.*, 1996; Neuwald *et al.*, 1999; Vale, 2000; Ogura & Wilkinson, 2001). In principle, two classes of Clp/Hsp100 proteins can be distinguished: class 1 proteins such as ClpA, ClpB/Hsp104 and ClpC consist of two distinct but conserved Walker-type nucleotide-binding domains (NBD), while class 2 proteins such as bacterial ClpX and ClpY (HslU) contain only a single NBD that is sufficient for function (Schirmer *et al.*, 1996). Unlike other class 1 proteins, however, members of the ClpB/Hsp104 family have a longer middle region or 'linker' that separates the two NBDs. This ClpB/Hsp104-linker is essential for chaperone activity (Cashikar *et al.*, 2002), but its precise structure and function is only poorly understood owing to the lack of a high-resolution crystal structure. Moreover, unlike other Clp/Hsp100 proteins, ClpB/Hsp104 does not associate with the structurally and functionally unrelated ClpP protease and does not direct the proteolytic degradation of its substrate proteins (Gottesman *et al.*, 1997; Horwich *et al.*, 1999; Wickner *et al.*, 1999; Dougan *et al.*, 2002). ClpB/Hsp104 rather functions exclusively as a molecular chaperone by facilitating the disaggregation of stress-damaged proteins (Sanchez & Lindquist, 1990; Sanchez *et al.*, 1992; Parsell *et al.*, 1994; Mogk *et al.*, 1999). The full recovery of these proteins requires the assistance of the cognate DnaK/Hsp70 chaperone system (Glover & Lindquist, 1998; Goloubinoff *et al.*, 1999; Mogk *et al.*, 1999; Motohashi *et al.*, 1999; Zolkiewski, 1999).

Currently, little is known about the structure–function relationship of ClpB/Hsp104 molecular chaperones. The crystal structure of an isolated N-terminal domain and that of NBD1 of *Escherichia coli* ClpB (Li & Sha, 2002, 2003) have been determined recently. While these structures have provided the first insight into this remarkable molecular machine, the structure of the full-length protein and of its functional assembly remain elusive. To understand the structural basis for protein disaggregation, we have crystallized full-length *T*ClpB in complex with AMPPNP and ATPγS, respectively.

2. Experimental

2.1. Expression, purification and crystallization of *T*ClpB

E. coli BL21 (DE3) cells were transformed with an expression plasmid (pMCB1) containing the *clpB* gene under control of the T7 RNA polymerase promoter (Motohashi *et al.*, 1999). Cells were grown at 310 K to mid-log phase in Luria–Bertani medium and induced by the addition of 1 m*M* isopropyl-β-D-thiogalactopyranoside (IPTG). The cells were grown for a further 3 h after induction and harvested by low-speed centrifugation at 277 K. For purification, the cell pellet was disrupted by passing through a microfluidizer processor (Microfluidics Corporation). *T*ClpB was purified from the supernatant by several column-chromatography steps in the following order: DEAE-Sepharose (BioRad), butyl-Sepharose (Tosohaas) and Mono-Q (Amersham Biosciences). After this process, the protein was judged to be greater than 98% pure by sodium dodecyl sulfate gel electrophoresis (data not shown). The purified protein was aliquoted and stored at 193 K.

Prior to crystallization, the protein was chromatographed on a Superose-6 size-exclusion column (Amersham Biosciences) to isolate the *T*ClpB hexamer and was concen-

trated to 15 mg ml^{-1} in 10 m*M* Tris–HCl pH 7.6, 100 m*M* NaCl, 10 m*M* $MgCl_2$ and 5% glycerol. The protein concentration was estimated by measuring the absorption at 280 nm in 6.0 *M* guanidine–HCl, 20 m*M* potassium phosphate buffer at pH 6.5 using a molar extinction coefficient of 57 180 M^{-1} cm^{-1} calculated by the method of Gill and von Hippel (1989). For crystallization, 5 m*M* AMPPNP or ATPγS were added directly to the protein sample. Native crystals (Fig. 1) were obtained at 291 K using the hanging-drop vapour-diffusion method by mixing 2 µl of protein sample with an equal volume of well solution consisting of 4–5%(*w*/*v*) polyethylene glycol 4000, 200 m*M* sodium acetate pH 4.1–4.3, 200 m*M* KCl and 20% glycerol. Crystals appeared after two to three weeks and reached maximum dimensions of 0.04 × 0.08 × 0.3 mm after two to three months.

2.2. X-ray crystallographic analysis of the crystals

Crystals were harvested into stabilizing solution consisting of 6%(*w*/*v*) polyethylene glycol 4000, 200 m*M* sodium acetate pH 4.1–4.3, 200 m*M* KCl and 20% glycerol and were transferred into a cryoprotectant solution consisting of stabilizing solution with a final glycerol concentration of 25%. The crystals were suspended in small nylon loops at the end of Hampton mounting pins (Hampton Research) and flash-frozen by plunging into liquid nitrogen.

Data were processed and scaled using the *HKL* software package (Otwinowski & Minor, 1997) and analyzed using *CNS* (Brünger *et al.*, 1998) and the *CCP*4 suite of programs (Collaborative Computational Project, Number 4, 1994).

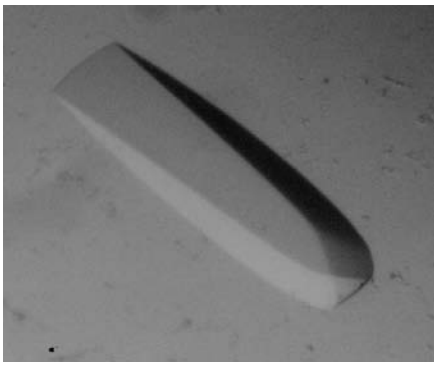

Figure 1
Crystals of full-length *T*ClpB in complex with AMPPNP.

3. Results and discussion

A number of different crystal forms were obtained, which all diffracted poorly (data not shown). After extensive screening of potential crystallization conditions, we obtained crystal forms of *T*ClpB (Fig. 1) which diffracted to 3.2 Å (AMPPNP) and 3.6 Å resolution (ATPγS), respectively, using synchrotron radiation (Table 1). Complete native data sets were collected at NSLS beamline X25 and were used for preliminary crystallographic analysis.

A self-rotation function was calculated using the *REPLACE* program (Tong & Rossmann, 1990). The self-rotation function revealed the existence of a single sixfold rotational axis along the crystallographic twofold screw axis parallel to *a* (Fig. 2). It is possible that the observed sixfold rotational

Table 1
Statistics of the native data sets for *T*ClpB.

Values in parentheses are for the highest resolution shell.

Type	Native	Native
Space group	$P2_12_12_1$	$P2_12_12_1$
Source	NSLS X25	NSLS X25
Wavelength (Å)	1.10	1.10
Detector type	B4 CCD 2K × 2K Brandeis	Quantum 4 ADSC
Resolution (Å)	48.8–3.2 (3.3–3.2)	49.2–3.6 (3.7–3.6)
Unit-cell parameters (Å)		
a	109.2	109.2
b	139.6	139.0
c	213.0	210.5
Ligand	AMPPNP	ATPγS
No. reflections	215099	279835
No. unique reflections	52294	37661
Data completeness (%)	95.9 (70.4)	99.9 (100)
$I/\sigma(I)$	27.7	12.5
R_{sym}† (%)	3.6 (27.5)	4.5 (41.4)

† $R_{sym} = \sum_{hkl} |I(hkl) - \langle I(hkl)\rangle| / \sum_{hkl} I(hkl)$, where $\langle I(hkl)\rangle$ is the mean of the symmetry-equivalent reflections of $I(hkl)$.

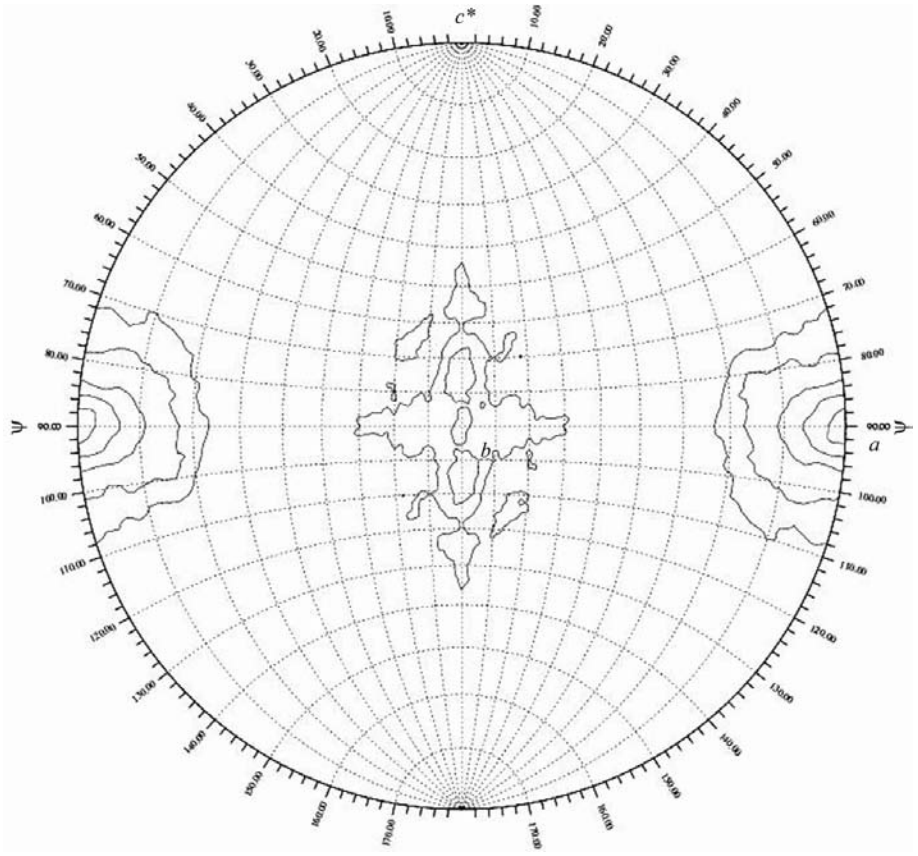

Figure 2
Stereographic projection of the self-rotation function with $\kappa = 60°$. The self-rotation function is contoured at the 1σ level with a 1σ cutoff. The resolution of the data used was 8–4 Å, with a radius of integration of 30 Å.

axis coincides with the crystallographic twofold screw axis, giving rise to a helical assembly with three molecules in the asymmetric unit. The presence of three molecules in the asymmetric unit would result in a V_M of 2.8 Å^3 Da^{-1}, corresponding to a solvent content of 55%, which is near the median of the commonly observed values of V_M (Matthews, 1968).

We thank Dr Y. Watanabe, Dr M. E. Sowa and J.-M. Choi for useful discussions, Dr T. Kawashima for help with data collection and the staff of NSLS X25 (Drs M. Becker, L. Berman and R. Sweet), APS-SBC 19ID (Dr A. Joachimiak) and MacCHESS (Dr D. Thiel) for access to and help with their respective synchrotron X-ray sources. SL acknowledges initial support by the Howard Hughes Medical Institute. FTFT is supported by a Scientist Development Grant from the American Heart Association (0130124N), a grant from the Robert A. Welch Foundation (Q-1530) and a grant from the Gillson Longenbaugh Foundation.

References

Brünger, A. T., Adams, P. D., Clore, G. M., DeLano, W. L., Gros, P., Grosse-Kunstleve, R. W., Jiang, J.-S., Kuszewski, J., Nilges, M., Pannu, N. S., Read, R. J., Rice, L. M., Simonson, T. & Warren, G. L. (1998). *Acta Cryst.* D**54**, 905–921.

Cashikar, A. G., Schirmer, E. C., Hattendorf, D. A., Glover, J. R., Ramakrishnan, M. S., Ware, D. M. & Lindquist, S. L. (2002). *Mol. Cell*, **9**, 751–760.

Collaborative Computational Project, Number 4 (1994). *Acta Cryst.* D**50**, 760–763.

Dougan, D. A., Mogk, A. & Bukau, B. (2002). *Cell. Mol. Life Sci.* **59**, 1607–1616.

Gill, S. C. & von Hippel, P. H. (1989). *Anal. Biochem.* **182**, 319–326.

Glover, J. R. & Lindquist, S. (1998). *Cell*, **94**, 73–82.

Goloubinoff, P., Mogk, A., Zvi, A. P., Tomoyasu, T. & Bukau, B. (1999). *Proc. Natl Acad. Sci. USA*, **96**, 13732–13737.

Gottesman, S., Wickner, S. & Maurizi, M. R. (1997). *Genes Dev.* **11**, 815–823.

Horwich, A. L., Weber-Ban, E. U. & Finley, D. (1999). *Proc. Natl Acad. Sci. USA*, **96**, 11033–11040.

Li, J. & Sha, B. (2002). *J. Mol. Biol.* **318**, 1127–1137.

Li, J. & Sha, B. (2003). *Structure*, **11**, 323–328.

Matthews, B. W. (1968). *J. Mol. Biol.* **33**, 491–497.

Mogk, A., Tomoyasu, T., Goloubinoff, P., Rüdiger, S., Röder, D., Langen, H. & Bukau, B. (1999). *EMBO J.* **18**, 6934–6949.

Motohashi, K., Watanabe, Y., Yohda, M. & Yoshida, M. (1999). *Proc. Natl Acad. Sci. USA*, **96**, 7184–7189.

Neuwald, A. F., Aravind, L., Spouge, J. L. & Koonin, E. V. (1999). *Genome Res.* **9**, 27–43.

Ogura, T. & Wilkinson, A. J. (2001). *Genes Cells*, **6**, 575–597.

Otwinowski, Z. & Minor, W. (1997). *Methods Enzymol.* **276**, 307–326.

Parsell, D. A., Kowal, A. S., Singer, M. A. & Lindquist, S. (1994). *Nature (London)*, **372**, 475–478.

Sanchez, Y. & Lindquist, S. (1990). *Science*, **248**, 1112–1115.

Sanchez, Y., Taulien, J., Borkovich, K. A. & Lindquist, S. (1992). *EMBO J.* **11**, 2357–2364.

Schirmer, E. C., Glover, J. R., Singer, M. A. & Lindquist, S. (1996). *Trends Biochem. Sci.* **21**, 289–296.

Tong, L. & Rossmann, M. G. (1990). *Acta Cryst.* A**46**, 783–792.

Vale, R. D. (2000). *J. Cell Biol.* **150**, F13–F19.

Wickner, S., Maurizi, M. R. & Gottesman, S. (1999). *Science*, **286**, 1888–1893.

Zolkiewski, M. (1999). *J. Biol. Chem.* **274**, 28083–28086.